Syntaxin4-Munc18c Interaction Promotes Breast Tumor Invasion and Metastasis by Regulating MT1-MMP Trafficking

Megan I. Brasher[1], Shawn C. Chafe[2], Paul C. McDonald[2], Oksana Nemirovsky[2], Genya Gorshtein[1], Zachary J. Gerbec[2], Wells S. Brown[2], Olivia R. Grafinger[1], Matthew Marchment[1], Esther Matus[1], Shoukat Dedhar[2,3], and Marc G. Coppolino[1]

ABSTRACT

Invasion of neighboring extracellular matrix (ECM) by malignant tumor cells is a hallmark of metastatic progression. This invasion can be mediated by subcellular structures known as invadopodia, the function of which depends upon soluble *N*-ethylmaleimide-sensitive factor-activating protein receptor (SNARE)-mediated vesicular transport of cellular cargo. Recently, it has been shown the SNARE Syntaxin4 (Stx4) mediates trafficking of membrane type 1–matrix metalloproteinase (MT1-MMP) to invadopodia, and that Stx4 is regulated by Munc18c in this context. Here, it is observed that expression of a construct derived from the N-terminus of Stx4, which interferes with Stx4-Munc18c interaction, leads to perturbed trafficking of MT1-MMP, and reduced invadopodium-based invasion *in vitro*, in models of triple-negative breast cancer (TNBC). Expression of Stx4 N-terminus also led to increased survival and markedly reduced metastatic burden in multiple TNBC models *in vivo*. The findings are the first demonstration that disrupting Stx4-Munc18c interaction can dramatically alter metastatic progression *in vivo*, and suggest that this interaction warrants further investigation as a potential therapeutic target.

Implications: Disrupting the interaction of Syntaxin4 and Munc18c may be a useful approach to perturb trafficking of MT1-MMP and reduce metastatic potential of breast cancers.

Introduction

Metastatic cancer remains largely incurable due to its systemic nature and resistance to therapeutic agents (1–3), with over 90% of mortality from cancer being attributable to metastatic disease (4). Triple-negative breast cancer (TNBC) in particular is often aggressive, resistant to treatment, and prone to metastasis (5, 6), highlighting a critical need for novel therapeutic strategies. The metastatic cascade begins with local invasion of neighboring extracellular matrix (ECM) and stromal cell layers by malignant cells (7). Growing evidence suggests that tumor cell invasion can be mediated by subcellular structures known as invadopodia (4, 8). Invadopodia are F-actin–rich membrane protrusions that facilitate matrix metalloproteinase (MMP)-mediated degradation of ECM components such as fibronectin, collagen, and laminin (9). Invadopodia have been studied in a variety of microenvironments *in vitro* (10–13), and there is also substantial evidence from *in vivo* studies that supports their role in the dissemination of tumor cells (14–16).

Delivery of proteins to invadopodia is necessary for their formation and function during tumor cell invasion (17). Vesicular transport of cellular cargo is dependent on soluble *N*-ethylmaleimide-sensitive factor-activating protein receptors (SNARE; ref. 18), and has been shown to play a role in invadopodia formation by facilitating the trafficking of membrane type 1–matrix metalloproteinase (MT1-MMP; refs. 19, 20) and EGFR to the cell surface (21). SNAREs are found on cargo-carrying vesicles (v-SNARE) and target membranes (t-SNARE; ref. 22), and fusion of these membranes requires the formation of a *trans*-SNARE complex between them. The *trans*-SNARE complex is formed through the interaction of the SNARE domains of v-SNAREs and t-SNAREs (18), allowing for delivery of cargo and membrane proteins. Previous research has indicated that the SNAREs SNAP23, VAMP7, VAMP3, Syntaxin13, and Syntaxin4 (Stx4) are involved in invadopodium formation, including trafficking of MT1-MMP (19, 20).

The molecular mechanisms by which SNARE activity is regulated represent important aspects of cargo trafficking that could be targeted to interfere with invadopodium-based degradation of ECM. Regulation of the plasma membrane SNARE Stx4 by Munc18c has been shown to facilitate trafficking of MT1-MMP and EGFR during invadopodium formation, and to support cell invasion of ECM, and is thus an attractive target for potential mitigation of MT1-MMP–dependent metastatic progression (21). Munc18c belongs to the Sec1/Munc18 (SM) family of proteins, which regulates membrane fusion by binding cognate SNAREs (23). Munc18c binds to the N-terminal region of Stx4 and regulates vesicle trafficking involving Stx4-containing complexes. We have previously shown that a GFP-tagged peptide containing the N-terminal 29 amino acids of Stx4 can be exogenously expressed in cells, bind to Munc18c (24), and perturb endogenous SNARE complex formation between SNAP23, VAMP2, and Stx4 (21). Intriguingly, using this peptide construct to block Stx4-Munc18c interaction in MDA-MB-231 breast adenocarcinoma cells also impaired gelatin degradation and cell invasion *in vitro*.

[1]Department of Molecular and Cellular Biology, University of Guelph, Guelph, Ontario, Canada. [2]Department of Integrative Oncology, BC Cancer Research Institute, Vancouver, British Columbia, Canada. [3]Department of Biochemistry and Molecular Biology, Faculty of Medicine, The University of British Columbia, Vancouver, British Columbia, Canada.

M.I. Brasher and S.C. Chafe contributed equally to this article.

Corresponding Author: Marc G. Coppolino, Department of Molecular and Cellular Biology, University of Guelph, 50 Stone Road East, Guelph, Ontario N1G 2W1, Canada. E-mail: mcoppoli@uoguelph.ca

Mol Cancer Res 2022;20:434–45

doi: 10.1158/1541-7786.MCR-20-0527

While expression of a construct containing amino acids 1 to 29 of Munc18c (Munc18c-N-term) can interfere with Stx4-Munc18c interaction, it has also been shown that the eighth amino acid (leucine) of Stx4 is required for Stx4 binding of Munc18c *in vitro* (24). This prompted examination of smaller fragments of the Stx4 N-terminus region for effects on Stx4-Munc18c binding, Stx4 function, and cell-ECM interactions. Here, we report that expression of residues 1 to 15 of the Stx4 N-terminus (Stx4-N-term-1–15) in TNBC cell lines perturbed trafficking of MT1-MMP, inhibited invadopodium formation, and reduced their invasive capacity *in vitro*. Furthermore, expression of truncated forms of Stx4 in TNBC cells *in vivo* also led to increased survival and reduced metastatic burden in spontaneous and experimental models of metastasis. These findings suggest that disrupting the interaction of Stx4 with Munc18c can dramatically alter metastatic behavior of cancer cells *in vivo*, and that targeting this interaction warrants further investigation for therapeutic potential.

Materials and Methods

Antibodies, plasmids, and reagents

Reagents and chemicals were purchased from either Fisher Scientific Ltd. or Millipore Sigma unless otherwise indicated. Antibody to Stx4 (610439) was from BD Biosciences. Antibodies to MT1-MMP, GFP, SNAP23, and Munc18c (ab3644, ab78738, ab4114, and ab175238) were from Abcam. Antibodies to Munc18c and EGFR (sc-373813 and sc-03) were from Santa Cruz Biotechnology. Antibodies to β_1 integrin, β tubulin, and GAPDH (P4C10, E7-s, and DSHB-hGAPDH-2G7) were from Developmental Hybridoma Studies Bank. Antibody to FLAG (F3165) was from Millipore Sigma. All fluorescently labeled secondary antibodies and Alexa Fluor 647-conjugated phalloidin were purchased from Life Technologies. MT1-MMP inhibitors MAB3329 and NSC 405020 were purchased from Millipore Sigma and Tocris Biotechne, respectively. GFP-Stx4-FL and Stx4-N-terminal peptide was cloned as described previously (21). Stx4 1 to 15 and Stx4 15 to 29 were purchased from Invitrogen GeneArt Gene Synthesis, and subcloned into pEGFP-N1 using KpnI and HindIII restriction enzyme sites. MT1-MMP 3xFLAG and MT1-MMP T567E 3xFLAG were subcloned from pEGFP-N1, as described previously (25), into pCDNA 3.1 3xFLAG using BamHI and HindIII restriction enzyme sites.

Cell lines

MDA-MB-231, MDA-MB-468, and $4T1^{luc}$ (26) cells were obtained from the ATCC and authenticated using short tandem repeat DNA profiling by a commercial testing facility (Genetica). Cells were cultured in DMEM supplemented with 10% bovine calf serum (BCS) or 10% FBS, and maintained at 37°C with humidity and a 5% CO_2 atmosphere. Cultures were routinely tested for *Mycoplasma* using LookOut *Mycoplasma* PCR detection kit (Millipore Sigma), or MycoAlert *Mycoplasma* detection kit (Lonza), and confirmed negative. Cells were lifted using 5 mmol/L EDTA/PBS (pH 7.4). Cells used in experiments were passaged between five and 20 times, and were passaged a maximum of 24 hours prior to each experiment. Cells were transfected with GFP-Stx4-FL, GFP-Stx4-N-term, pEGFP-N1 alone (GFP control), GFP-Stx4 1 to 15, and GFP-Stx4 15 to 29. —One to 15 and 15 to 29 from Stx4 was purchased through Thermo Fisher Scientific GeneArt subcloning and express cloning service and were cloned into pEGFP-N1 using the following oligonucleotides as primers: forward Stx4-1-15 (5′TGACGGTAAATGGCCCGCCTGGC ATTATG-3), reverse Stx4-1-15 (5′-TTCACGAATCCTTACT-TGTACAGCTCGTCCATGC CGAGA-3′), forward Stx4-15–29 (5′-TTCACGGATCCATGTCGGACGAAGAGGACAAGGA GCGGG-3′), and the same reverse primer as Stx4-1-15. Stable cell lines were created as previously described (21), with the addition of two new stable cell lines expressing GFP-Stx4 1 to 15 and GFP-Stx4 15 to 29. Cells were transfected using jetPRIME Polyplus (VWR International) according to the protocol of the manufacturer. All transiently transfected constructs were expressed for 24 hours.

Protein analyses

Cells were lysed *in situ* with cold lysis buffer comprising 1% Nonidet P-40, 10% glycerol, 0.5% deoxycholate, 137 mmol/L NaCl, 20 mmol/L Tris-HCl (pH 8.0), 10 mmol/L NaF, 10 mmol/L $Na_2P_4O_7$, 0.2 mmol/L Na_3VO_4, and protease inhibitor mixture (Sigma). Coimmunoprecipitation was performed as previously described (21). Total protein levels in lysates were determined through a Bradford protein assay (Bio-Rad). Values used for densitometry were obtained using ImageJ software's analyze gel feature. All bands analyzed were calculated relative to loading control bands.

Invadopodium formation assay

Invadopodium formation was performed as previously described (19). Glass coverslips were coated with 50 μg/mL poly-L-lysine (PLL)/PBS, followed by cross-linking with 0.5% glutaraldehyde/PBS. Coverslips were then inverted onto 70 μL of Alexa Fluor 594-labeled gelatin. The coated coverslips were then incubated with 5 mg/mL $NaBH_3$/PBS and subsequently washed with PBS. All images of cells plated on fluorescent gelatin for invadopodium formation were incubated on gelatin for 8 hours instead of 4 hours to allow for degradation that could be easily captured by confocal microscopy. Tissue culture plates were coated similarly, the exception being that plates were coated with 0.2% unlabeled gelatin/PBS. MT1-MMP–mediated ECM degradation was suppressed using 50 μmol/L NSC405020 and the MT1-MMP blocking antibody was used at a concentration of 2 μg/mL, as described previously (12).

Gelatin degradation assay

Gelatin degradation assays were performed as described previously (27). Briefly, coverslips were coated with Alexa Fluor 594-labeled gelatin as described under "invadopodium formation assay". Cells were seeded at 30% confluency and incubated for 24 hours. Degradation areas made by transfected cells were counted and scored as the percentage of area degraded per cell (+1 for fully degraded, +0.5 for partially degraded, and 0 for no degradation).

Confocal immunofluorescence microscopy

Cells were grown on glass coverslips for 4 hours or 24 hours (as described under "invadopodium formation assay"). Cells were fixed in 4% paraformaldehyde/PBS and then washed in 150 mmol/L glycine/PBS at room temperature with gentle agitation. Cells were permeabilized in 0.1% Triton X-100/PBS and blocked in 5% BSA/PBS prior to staining with primary and secondary antibody. Samples analyzed by confocal microscopy were imaged through a 63x (numerical aperture 1.4) oil immersion lens using a Leica DM-IRE2 inverted microscope with a TCS SP2 scanning head (Leica). Images were captured using Leica confocal software. All images were processed and analyzed using ImageJ software (NIH, Bethesda, MD).

Cell invasion assay

Cell culture inserts were prepared as described previously (28). Briefly, the bottom of transwell inserts (8-μmol/L pore diameter; Corning Inc.) were coated with 20 μg/mL fibronectin/PBS and the

tops with 0.125 mg/mL Matrigel (BD Biosciences). Parental and stable cells were serum-starved for 24 hours, lifted, seeded into chambers, and allowed to invade for 20 hours. The cells that invaded towards the lower chamber (10% BCS/0.1% BSA in DMEM) were fixed in 4% paraformaldehyde, stained with Hoescht, and counted. Cells that did not invade were removed with a cotton swab prior to fixation of the sample. Ten fields of cells per membrane were counted per treatment. Data are presented as percent of control.

Cell surface protein labeling

Cells were plated onto 0.2% gelatin (as described under "invadopodium formation assay") for 4 hours. Cells were then washed with cold PBS once and incubated with 0.5 mg/mLSulfo-NHS-SS-Biotin (APExBIO) dissolved in 10 mmol/L boric acid and 150 mmol/L NaCl (pH 8.0) at 4°C with occasional agitations. Plates were then washed with 15 mmol/L glycine/PBS and lysed (as described under "protein analysis").

Statistical analysis

The percent of controls for three experimental replicates is shown, with error bars representing the SD. The horizontal bar for each treatment indicates the mean, in all graphs, unless otherwise indicated. For all experiments, each experimental group was compared with its respective control, vehicle, or wild-type treatment by ANOVA with Bonferroni posthoc analysis using a Tukey posthoc analysis. Survival analyses were performed by the Kaplan–Meier method and compared by the log-rank test. Longitudinal tumor growth analyses by ANOVA with Bonferroni correction were performed using TumGrowth (29). All statistical analyses were performed using Excel and GraphPad Prism v7.0. P values < 0.05 were considered significant.

Animal studies

All animal studies and procedures were performed in accordance with protocols approved by the Institutional Animal Care Committee at the BC Cancer Research Institute and University of British Columbia (Vancouver, BC, Canada) under approved protocol A18–0132. For human tumor xenograft studies, 1×10^6 MDA-MB-231 cells expressing Stx4—full-length (Stx4-FL), Stx4-N-term, or Stx4-Cyto were injected into the left fourth mammary gland in a solution of 50% Matrigel and 50% saline. Tumor growth was monitored by digital caliper and volumes were calculated using the modified ellipsoid formula ($L \times W^2 \times \pi/6$). To plot survival a surrogate endpoint volume of 400 mm^3 was utilized for survival events. The study proceeded until mice in one of the study cohorts became moribund, at which time the group was culled. Remaining groups in the study were allowed to have their average tumor volume match that of the initial group culled so as to evaluate metastatic burden independently of primary tumor volume. For experimental metastasis assays, $4T1^{luc}$-derived cell lines, stably expressing Stx4-FL, Stx4-cyto, or Stx4-N-term constructs, were injected (5×10^5 cells/injection in 100 μl saline) into the lateral tail vein of 7- to 9-week-old female BALB/c mice (The Jackson Laboratory). Mice were imaged once per week and weighed three times weekly to follow the growth of metastases. Mice were injected intraperitoneally with 150 mg/kg D-luciferin (PerkinElmer) 10 minutes prior to imaging. Bioluminescent images were captured on an IVIS Spectrum. Bioluminescent signal of lung metastatic burden was quantified in Living Image. To evaluate differences in metastatic propensity among the Stx4 constructs, all mice were euthanized when mice in one group became moribund.

IHC and histochemical staining of tissues

Tumors and lungs were removed and placed in 10% neutral buffered formalin. Formalin-fixed paraffin-embedded tissues were dewaxed in xylene, gradually rehydrated in ethanol baths of decreasing ethanol concentration, and incubated in PBS. Antigen retrieval was performed by incubation in 0.01 mol/L citrate, pH 4.0 by microwaving on high for 10 minutes. Lung sections were then stained with antibody to vimentin (BD Biosciences 550513; 1:200) overnight and incubated with species-specific secondary antibody (ImmPRESS HRP Universal antibody Vector Laboratories; MP-7500) the following morning according to the manufacturer's instructions. Detection was performed using the DAB peroxidase (horseradish peroxidase; HRP) substrate kit (Vector Laboratories; SK-4100). Histochemical evaluation was done by hematoxylin and eosin (H&E) staining. Lung sections from 5 mice from each group were evaluated. Whole tissue scans were performed on a Panoramic Midi (3D Histec) using a 20x objective. Metastatic burden was calculated for entire lung sections using *Case Viewer* (3D Histech) to draw region of interest (ROI) around vimentin-positive clusters, summing the area of the ROIs (μm^2), and dividing by the total area (μm^2) for the section (30).

Results

Expression of an N-terminal fragment of Stx4 (a.a. 1 to 15) impairs formation of endogenous Stx4-containing SNARE complexes

It has recently been shown that expression of a GFP-tagged construct comprising the initial 29 N-terminal amino acids of Stx4 (Stx4-N-term) causes a decrease in SNARE complex formation involving endogenous Stx4, SNAP23, and VAMP2 (21). It has also been found that the binding of Munc18c to Stx4 requires leucine 8 of Stx4 (24). We therefore generated GFP-tagged constructs comprising full-length Stx4, amino acids 1 to 15 of Stx4, or amino acids 15 to 29 of Stx4 to study the effect of expression of these fragments on SNARE complex formation and invadopodium-based cell invasion. MDA-MB-231 cells were used to derive stable cell lines expressing these constructs, and the ability of the constructs to associate with endogenous Munc18c was examined by coimmunoprecipitation. Munc18c was found to coimmunoprecipitate with GFP-Stx4 1 to 15, but not GFP-Stx4 15 to 29 (**Fig. 1A**). The effect of expressing Stx4 constructs on SNARE complex formation was examined by immunoprecipitating Stx4 cognate binding partner SNAP23. Cells expressing GFP-Stx4-1–15 had a dramatic decrease in the amount of Stx4 associated with SNAP23, compared with control cells expressing no construct (parental) or GFP-Stx4-FL (**Fig. 1B** and **C**). Expression of GFP-Stx4-FL did appear to promote, modestly, SNARE complex formation, which may result from stimulation of trafficking caused by overexpression of functional Stx4. Consistent with previous findings, cells expressing GFP-Stx4-N-term also had a significant decrease in the amount of Stx4 associating with SNAP23 (**Fig. 1B** and **C**; ref. 21). This effect was not observed in cells expressing GFP-Stx4-15–29. These results indicate that expression of a fragment of Stx4′s N-terminal region fragment, containing amino acids 1 to 15, can impede the ability of Stx4 to form complexes with endogenous SNARE partners.

Expression of Stx4-1–15 impairs invadopodium formation and gelatin degradation

It was previously observed that expression of Stx4-N-term in MDA-MB-231 cells inhibited invadopodium formation and gelatin degradation (21). Here, MDA-MB-231 cells, or MDA-MB-231–derived cells stably expressing GFP alone, GFP-Stx4-FL, GFP-Stx4-N-term, GFP-

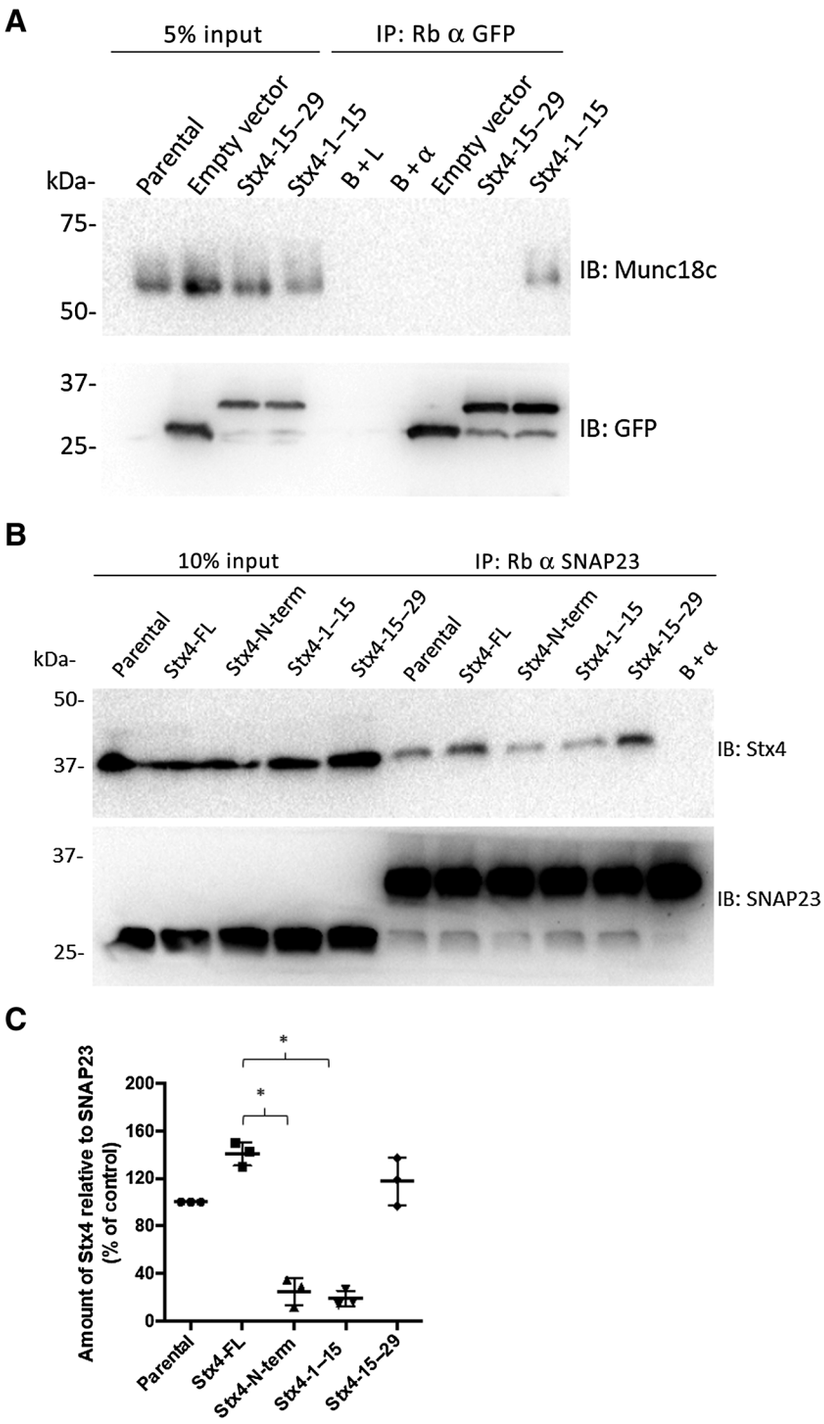

Figure 1.

Association of Stx4 1 to 15 with Munc18c inhibits Stx4–SNAP23 interaction. **A,** Parental MDA-MB-231 cells, and cell lines stably expressing GFP, GFP-Stx4-1-15, or GFP-Stx4-15-29 were lysed, and GFP was immunoprecipitated. Immunoprecipitates (IP) were probed for Munc18c. **B,** Parental MDA-MB-231 cells, and cells stably expressing Stx4-FL. Stx4–N-term, Stx4-1-15, or Stx4-15-29 were lysed, and SNAP23 was immunoprecipitated. IPs were probed for Stx4 and SNAP23. **C,** Densitometry of the amount of Stx4 coimmunoprecipitated relative to SNAP23 as shown in **B** (*, $P < 0.05$). Data represent three or more biological replicates with at least three technical replicates. B+α, beads plus antibody; B+L, beads plus GFP lysate. IB, immunoblot.

Stx4-1-15, or GFP-Stx4-15–29, were subjected to invadopodium formation and gelatin degradation assays. Cells were plated onto fluorescently labelled gelatin, for 4 or 24 hours, to study invadopodium formation and gelatin degradation, respectively (**Fig. 2A** and **B**). Cells expressing GFP-N-term showed an 85.79% ± 12.98% decrease in invadopodium formation, while cells expressing GFP-Stx4-1–15 showed an 89.51% ± 17.30% decrease, compared with control cells. The effect of expressing the Stx4 N-terminal domain on invadopodium formation was confirmed using another cell line derived from metastatic breast cancer, MDA-MB-468. Expression of GFP-Stx4-N-term in MDA-MB-468 cells resulted in a 75.94 ± 6.08% decrease in invadopodium formation (**Fig. 2C**).

MDA-MB-231 cells expressing GFP-Stx4-N-term exhibited a 76.80% ± 10.60% decrease in gelatin degradation, while expression of GFP-Stx4-1-15 led to an 83.51% ± 2.37% decrease, compared with control cells (**Fig. 2C**). There was no significant decrease in

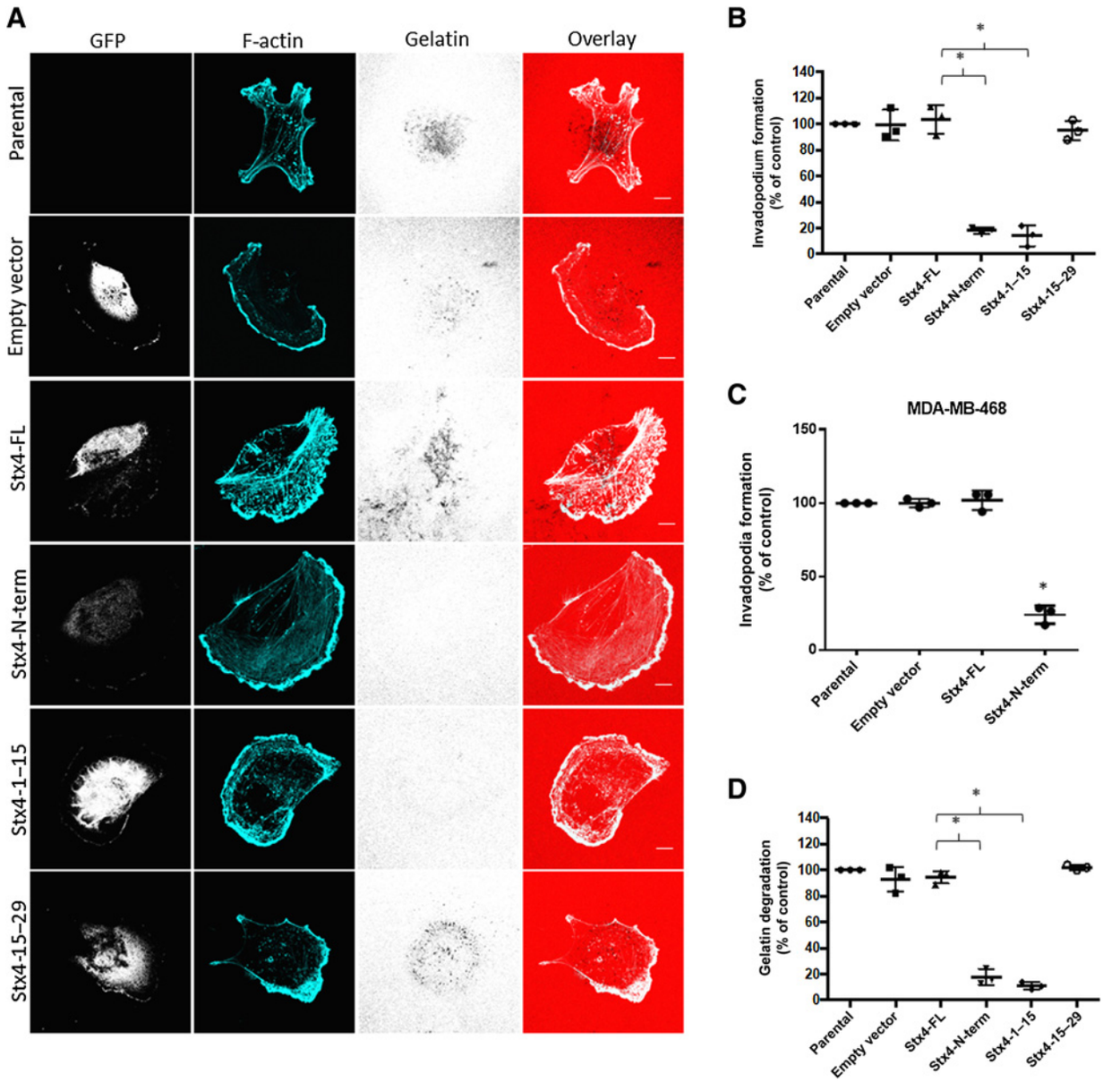

Figure 2.

Expression of Stx4 1 to 15 impairs invadopodium formation and gelatin degradation. **A,** Invadopodium-based degradation of gelatin by cells expressing GFP (control), Stx4-FL, Stx4–N-term, Stx4-1–15, or Stx4-15–29. Cells were seeded onto fluorescent gelatin for 4 hours, and then fixed, permeabilized, stained for F-actin, and analyzed by confocal microscopy. Scale bars = 10 μm. **B,** Quantification of invadopodium formation. Cells were seeded onto fluorescent gelatin and processed as in **A**. Cells with F-actin puncta overlying dark spots of gelatin degradation were counted as cells forming invadopodia. Percentages of cells forming invadopodia, normalized to parental cells, were determined by counting 50 cells/sample. **C,** Invadopodium-based degradation of gelatin (as in **B**) by parental MDA-MB-468 cells, or those transiently expressing GFP, GFP-Stx4-FL, or GFP-Stx4-N-term. **D,** Cells, as in **A,** were seeded onto fluorescent gelatin for 24 hours, and then fixed. Dark areas representing degradation of gelatin were analyzed and scored as described under "Materials and Methods". All data are presented as percent of control ± SD. Asterisks denote values significantly different from control (*, $P < 0.05$). All data represent three or more biological replicates with at least three technical replicates.

invadopodium formation or gelatin degradation in cells expressing GFP-Stx4-15–29 (**Fig. 2D**).

Expression of Stx4-1-15 inhibits cell migration, invasion, and trafficking of MT1-MMP to the cell surface

Stx4 and SNAP23, along with VAMP2, contribute to the vesicle-mediated trafficking of MT1-MMP in MDA-MB-231 cells (19, 21). To assess the effects of disrupting the interaction of Stx4 and SNAP23 through expression of GFP-Stx4-1-15, we analyzed the trafficking of key invadopodial proteins during cell invasion. Cell surface levels of MT1-MMP, EGFR, and β_1 integrin were assessed by biotinylating cell surface proteins in cells plated on gelatin (**Fig. 3A** and **B**). While cell surface levels of β1-integrin were not significantly altered, the amounts of cell surface MT1-MMP and EGFR were decreased by 92.20% ±

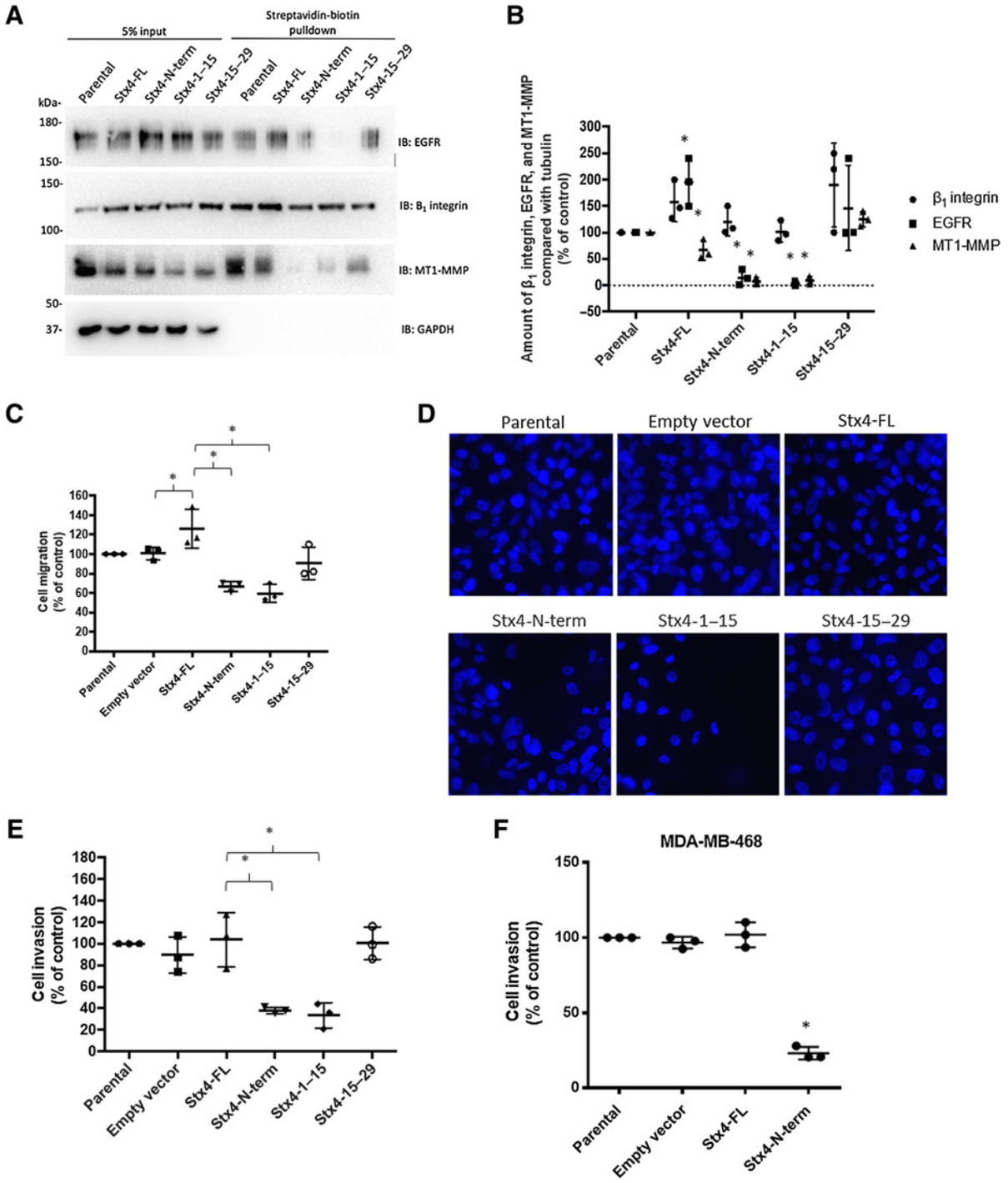

Figure 3.

Expression of Stx4-1–15 decreases cell surface levels of MT1-MMP and EGFR, as well as cell migration and invasion. **A,** Parental MDA-MB-231 cells and stable cell lines expressing Stx4-FL, Stx4-N-term, Stx4-1-15, and Stx4-15-29 were plated onto gelatin for 4 hours, exposed to biotin, and then lysed and analyzed by precipitation with streptavidin beads. Cell surface levels of β_1 integrin, MT1-MMP, and EGFR were assessed by Western blotting. GAPDH was used as a loading control. **B,** Densitometric analysis of the amounts of β_1 integrin, EGFR, MT1-MMP in streptavidin precipitates, as in **A,** relative to control. Cells, as in **A,** were serum-starved for 24 hours, and seeded onto uncoated membranes of transwell chambers, and allowed to migrate for 20 hours (**C**), or seeded onto Matrigel-coated membranes and allowed to invade for 24 hours (**D** and **E**). **D,** Representative images of DAPI stained cells that invaded through the Matrigel-coated membrane. Quantification of invasion in MDA-MB-231 (**E**) and MDA-MB-468 (**F**) cells. Parental cells, or those expressing GFP, GFP-Stx4-FL, or Stx4-N-term were serum-starved for 24 hours and seeded onto Matrigel-coated membranes and allowed to invade for 24 ours. In **C, E,** and **F,** percentages of cells are shown from experiments in which at least 10 fields of view were counted per treatment. All data represent percent of control ± SD, from three or more biological replicates, with at least three technical replicates; asterisks denote values significantly different from controls (*, $P < 0.05$). IB, immunoblot.

6.67% and 85.06% ± 15.13%, respectively, in cells expressing GFP-Stx4-N-term compared with control. Similarly, cell surface levels of MT1-MMP and EGFR were decreased by 57.53% ± 22.29% and 96.45% ± 3.86%, respectively, in cells expressing GFP-Stx4 1–15. Cells expressing GFP-Stx4-FL showed a less pronounced decrease in MT1-MMP levels of only 33.41% ± 18.73%, consistent with previous findings (21).

The ability of stable cell lines expressing GFP-Stx4 constructs to migrate and invade was examined using transwell migration assays and Matrigel-based invasion assays. Cells expressing GFP-Stx4-N-term displayed a 33.33% ± 0.71% and a 62.21% ± 3.13% decrease in cell migration (**Fig. 3C**) and invasion (**Fig. 3D** and **E**), respectively. Cells expressing GFP-Stx4-1-15 displayed 42.00% ± 6.24% and 66.33% ± 11.68% decreases in cell migration (**Fig. 3C**) and invasion (**Fig. 3D** and **E**), respectively. No significant difference was found between parental MDA-MB-231 cells, GFP-expressing cells, GFP-Stx4-FL-expressing cells, or GFP-Stx4-15–29-expressing cells. Consistent with our findings in MDA-MB-231 cells, MDA-MB-468 cells expressing GFP-Stx4-N-term exhibited a 76.91 ± 4.23% decrease in invasion (**Fig. 3F**).

Confirmation that invasion by the MDA-derived cell lines was MT1-MMP–dependent was obtained by treating cells with a combination of MT1-MMP inhibitor NSC405020 and an MT1-MMP-blocking antibody, MAB3329, which inhibits the catalytic domain of MT1-MMP (12). This treatment dramatically reduced invadopodium formation (**Fig. 4A**) and gelatin degradation (**Fig. 4B**) in parental MDA-MB-231 cells, as well as cells expressing GFP-Stx4-FL or GFP-Stx4-15–29. Detectable decreases in invadopodium formation and gelatin degradation were also observed in cells expressing GFP-Stx4-N-term and GFP-Stx4-1-15 (**Fig. 4A** and **B**). These findings are consistent with the notion that inhibiting the ability of Stx4 to form complexes with SNAP23, by expressing N-terminal fragments of Stx4, reduces invadopodia formation and ECM degradation by impairing the trafficking of MT1-MMP. The findings also suggest that a small percentage of MT1-MMP–dependent invadopodium-based gelatin degradation is not dependent on Stx4 function.

Expression of MT1-T567E increases invadopodium formation in cells expressing GFP-Stx4-N-term peptide and GFP-Stx4-1–15

Overexpression of a phosphomimetic mutant of MT1-MMP, MT1-MMP-T567E, has been shown to increase cell migration and invasion, through stimulation of MT1-MMP recycling and associated downstream signaling (25). We reasoned that expression of MT1-MMP-T567E might therefore increase gelatin degradation and invasion in cells expressing GFP-Stx4-N-term or GFP-Stx4-1–15. Cells were transfected with either MT1-MMP-3xFLAG or MT1-MMP-T567-E3xFLAG and plated onto fluorescent gelatin for 4 and 24 hours, respectively. Cells expressing MT1-MMP-T567E showed a significant increase in invadopodium formation (**Fig. 5A** and **B**) and gelatin degradation (**Fig. 5C**). Cells expressing GFP-Stx4-N-term showed a 200.48% ± 38.96% increase in invadopodium formation, and a 149.49% ± 26.42% increase in gelatin degradation, when MT1-MMP-T567E-3xFLAG was also expressed, compared with GFP-Stx4-N-term–expressing cells transfected with MT1-MMP-WT-3xFLAG. Similarly, cells expressing GFP-Stx4-1-15 peptide along with MT1-MMP-T567E-3xFLAG showed a 172.77% ± 32.09% increase in invadopodium formation, and a 191.72% ± 36.6% increase in gelatin degradation, compared with GFP-Stx4-1–15–expressing cells transfected with MT1-MMP-WT-3xFLAG.

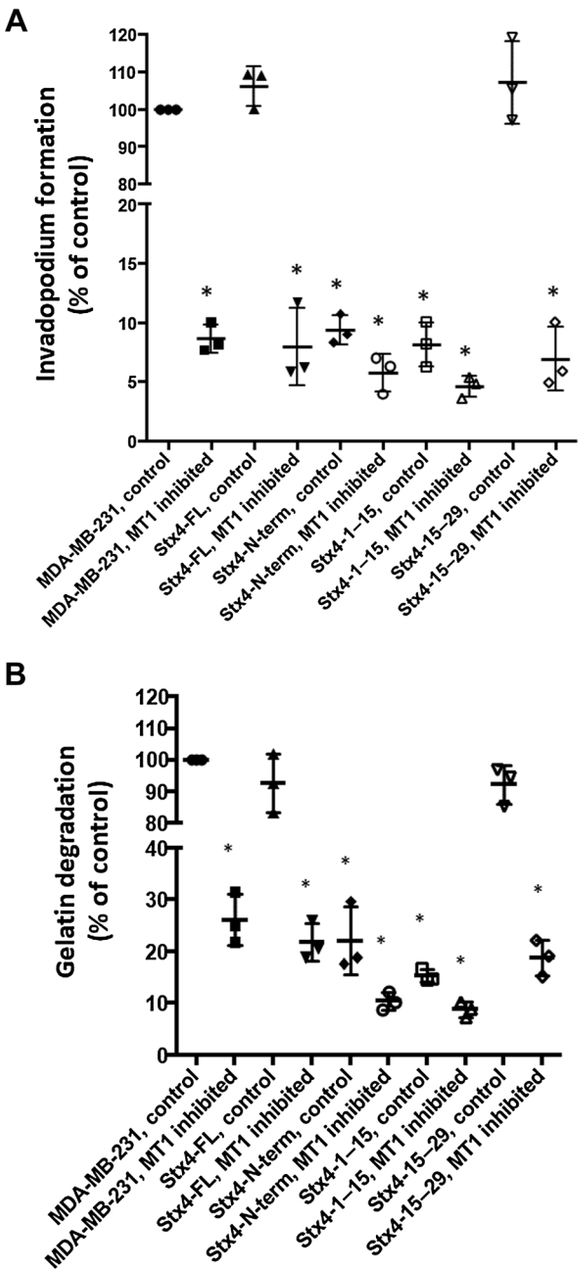

Figure 4.

Invadopodium formation and gelatin degradation in MDA-MB-231 cells is MT1-MMP–dependent. **A,** Parental MDA-MB-231 cells and stable cells expressing Stx4-FL, Stx4-N-term, Stx4-1–15, and Stx4-15–29 were treated with either DMSO (control) or MAB3329 and NSC405020, plated onto gelatin for 4 hours, then fixed, permeabilized, stained for F-actin, and analyzed by confocal microscopy. **B,** Cells, as in **A,** were plated onto gelatin for 24 hours, then fixed, permeabilized, stained for F-actin, and analyzed by confocal microscopy. Invadopodia (**A**) and gelatin degradation (**B**) were quantified as described in "Materials and Methods". Means ± SD are presented from three or more biological replicates, with at least three technical replicates; asterisks denoting values significantly different from controls (*, $P < 0.05$).

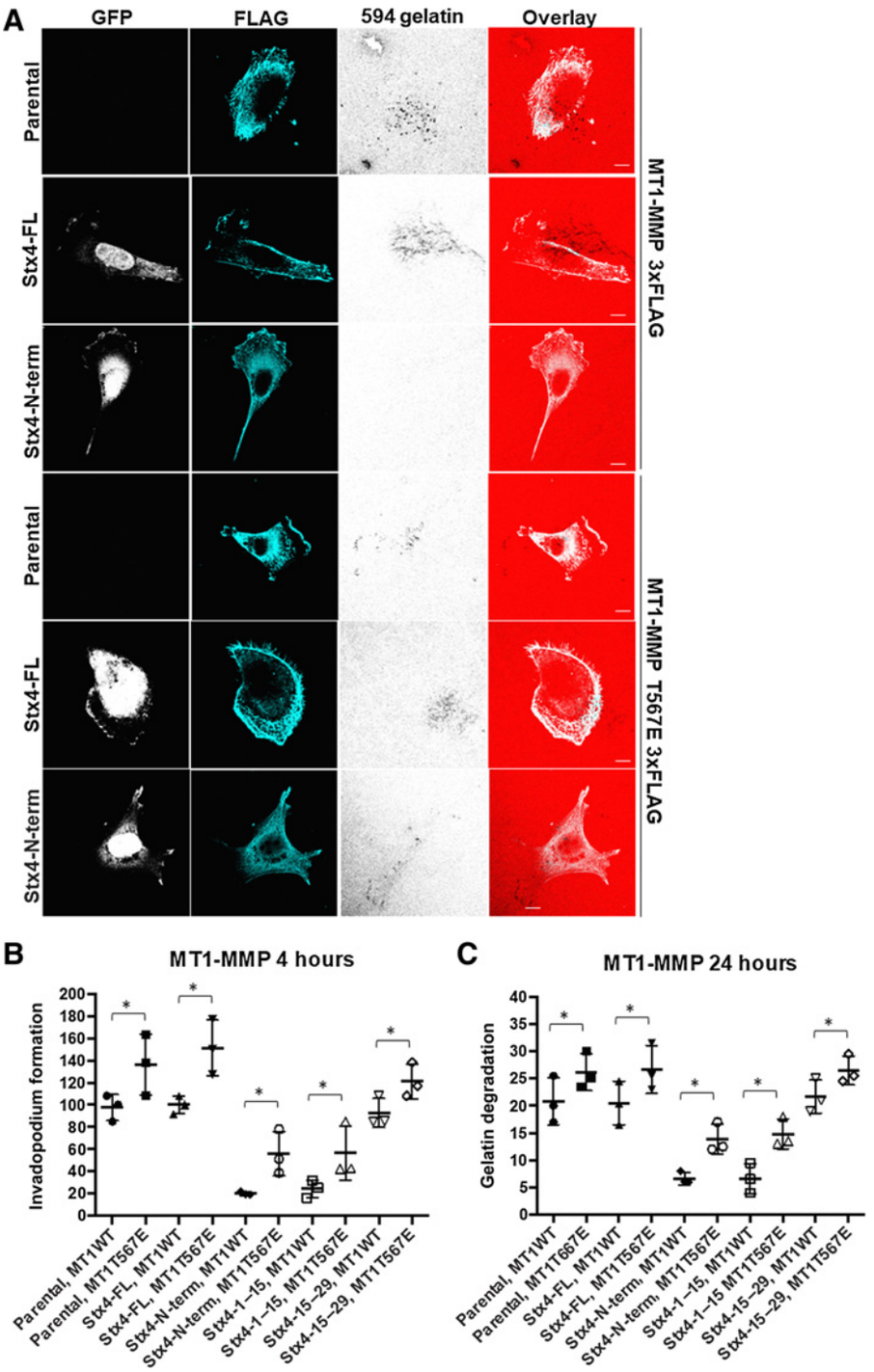

Figure 5.

Expression of MT1-MMP-T567E increases invadopodium formation and gelatin degradation in cells expressing Stx4-N-term or Stx4 1 to 15. **A,** Parental MDA-MB-231 cells and stable cells expressing Stx4-FL, Stx4-N-term, Stx4-1–15, and Stx4-15–29 were transfected with either MT1-MMP-WT-3xFLAG or MT1-MMP-T567E-3xFLAG for 20 hours, plated onto gelatin for 4 hours, then fixed, permeabilized, stained for F-actin, and analyzed by confocal microscopy. Cells, as in **A,** were plated onto gelatin for 4 hours (**B**), or 24 hours (**C**), then fixed, permeabilized, stained for F-actin, and analyzed by confocal microscopy. As described in "Materials and Methods", invadopodia (**B**) and gelatin degradation (**C**) were quantified. All data are presented as percent of control ± SD from three or more biological replicates with at least three technical replicates. Asterisks denote values significantly different from control (*, $P < 0.05$).

Expression of cytoplasmic segments of Stx4 in MDA-MB-231 cells reduces metastasis *in vivo*

The results above indicate that interfering with interaction of Stx4 and Munc18c cells impairs MT1-MMP–dependent invadopodium formation and gelatin degradation. To assess whether this has impact on metastatic potential *in vivo*, we orthotopically implanted MDA-MB-231 cells expressing truncated Stx4 constructs into immunocompromised mice. Similar to the Stx4-N-term construct, expression of the cytoplasmic domain of Stx4 (Stx4-cyto) has previously been shown to reduce invadopodium formation, gelatin degradation and invasion in MDA-MB-231 cells (19). Expression of Stx4-cyto or Stx4-N-term delayed tumor growth (**Fig. 6A**), and extended survival (**Fig. 6B**) relative to the expression of Stx4-FL. Weighing lungs upon necropsy revealed that lungs removed from both the Stx4-N-term and Stx4-Cyto tumor-bearing mice weighed significantly less than Stx4-FL tumor-bearing mice (**Fig. 6C**). To assess whether this was due to differences in

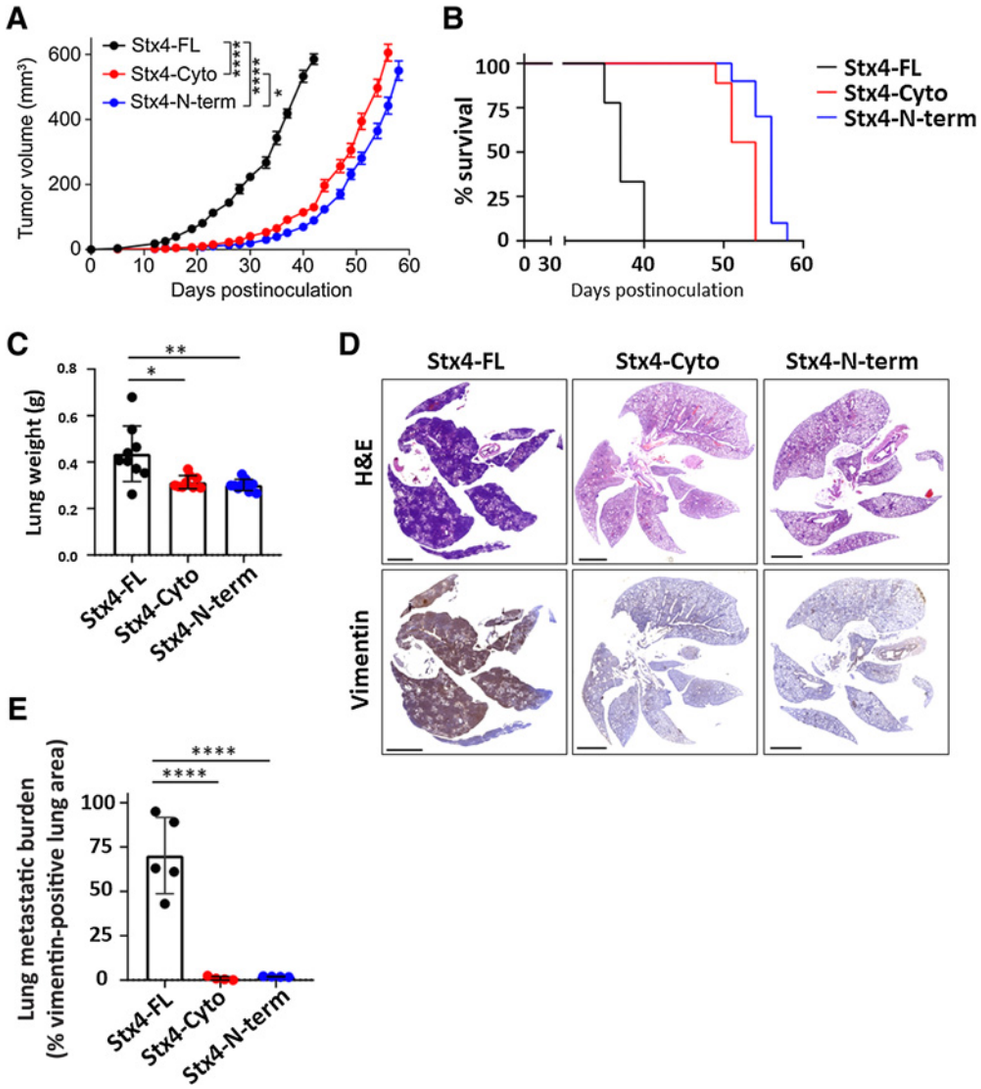

Figure 6.

Expression of truncated Stx4 constructs reduces spontaneous breast cancer metastasis. **A,** Tumor growth of orthotopically implanted MDA-MB-231 stable cells expressing Stx4-FL, Stx4-N-term, and Stx4-Cyto. **B,** Kaplan–Meier curves plotting surrogate survival of mice injected with cells in **A**. $N = 10$ mice/group. **C,** Wet lung mass (g) for individual mice for the indicated groups. **D,** Histochemical (H&E) and IHC (vimentin) evaluation of whole lung sections. $N = 5$ lungs/group; bar = 2,000 μm. **E,** Quantification of metastatic burden for the indicated groups. Symbols indicate total burden for individual mice. Asterisks denote significant differences. (*, $P < 0.05$; **, $P < 0.01$; ****, $P < 0.0001$).

metastatic burden, we stained lung sections with H&E and vimentin (ref. 30; **Fig. 6D**). Mice bearing Stx4-FL tumors had substantive metastatic growth in the lungs. In stark contrast, expression of Stx4-cyto or Stx4-N-term nearly completely abrogated the metastatic capacity of the MDA-MB-231 tumors, reducing metastatic burden by 98.7% and 97.3%, respectively (**Fig. 6E**).

To assess the impact of interfering with the interaction of Stx4-Munc18c on metastatic potential in another model of TNBC, in a setting that captures the latter steps of the metastatic cascade and assesses extravasation, which relies upon invadopodia formation (31), experimental metastasis assays were conducted using the luciferase-expressing murine breast cancer cell line $4T1^{luc}$. $4T1^{luc}$ cells stably expressing empty vector or Stx4 constructs (full length, cyto, and N-term) were developed, and consistent with MDA-MB-231 and MDA-MB-468 models, cells expressing Stx4-cyto or Stx4-N-term showed reduced invadopodium formation (**Fig. 7A**) and gelatin degradation (**Fig. 7B**) *in vitro*. To measure metastatic potential, stable $4T1^{luc}$ lines were injected intravenously and formation of lung metastases was monitored. Cells expressing either Stx4-cyto or Stx4-N-term had dramatically lower levels of lung metastases (**Fig. 7C** and **D**). Together with our observations in other cell types, and our *in vitro* findings, these data suggest that interfering with the Stx4-Munc18c interaction is an effective strategy to block metastasis.

Discussion

Observations from studies described here support the conclusion that MT1-MMP–driven invadopodium formation and metastasis in

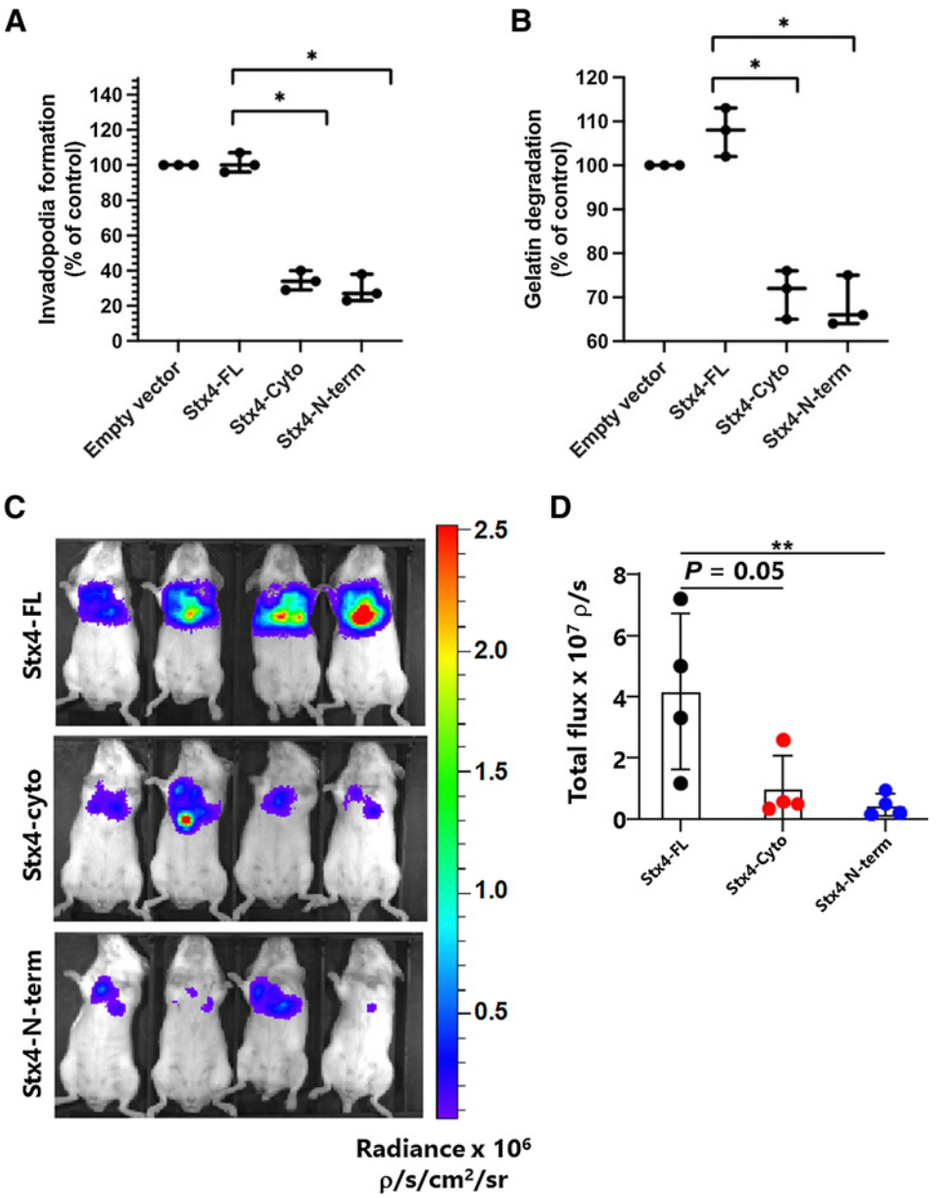

Figure 7.

Expression of truncated Stx4 constructs reduces invadopodia formation, gelatin degradation, and breast cancer metastasis. **A,** 4T1^{luc} cells stably expressing GFP (control), Stx4-FL, Stx4 Cyto, or Stx4–N-term were plated onto fluorescent gelatin for 4 hours (**A**) or 24 hours (**B**), then fixed and permeabilized. As described in "Materials and Methods", invadopodia (**A**) and gelatin degradation (**B**) were quantified. Percentages of cells forming invadopodia, normalized to GFP, were determined by counting 50 cells/sample. All data are presented as percent of control ± SD from three or more biological replicates with at least three technical replicates. Asterisks denote values significantly different from control (*, $P < 0.05$). **C,** BALB/c mice were inoculated intravenously via the lateral tail vein with 5×10^5 4T1-luciferase cells stably expressing the indicated Stx4 construct, and lung metastases were imaged 3 weeks postinjection via IVIS. **D,** Bioluminescent emission from the thoracic region was calculated and quantified. Data are shown for individual mice. Statistical significance was calculated via one-way ANOVA, (**, $P < 0.01$).

TNBC are regulated by the interaction of Syntaxin4 and Munc18c. This conclusion is based on the following findings: expression of constructs containing portions of the N-terminus of Stx4 (i) decreases the formation of Stx4-containing SNARE complexes; (ii) perturbs delivery of MT1-MMP to the plasma membrane, inhibits formation of invadopodia and cell invasion, *in vitro*, in MDA-MB-231 and MDA-MB-468 cells; (iii) reduces the metastatic progression of orthotopic MDA-MB-231 tumors in mouse xenografts; and (iv) reduces metastasis *in vivo* in a 4T1^{luc} model of experimental metastasis. These results are consistent with previous studies indicating the importance of invadopodia for cancer cell extravasation *in vivo* (31). In the future, it will be ideal to test the Stx4-1-15 construct *in vivo*, and we are currently working to optimize an approach to this. The findings here, to our knowledge, are the first *in vivo* demonstration of a role for SNARE/Munc18c-regulated trafficking in tumor progression.

SNAREs have previously been shown to play key roles in invadopodium formation, cell migration, and MMP-mediated ECM degradation (19–21, 25, 28); however, there is little information defining how SNAREs are regulated during these processes. Munc18c has been characterized as both a positive (24, 32, 33) and negative regulator (34, 35) of Stx4, and here we demonstrate that disrupting Stx4-Munc18c interaction decreases Stx4 association with cognate SNARE partners, and reduces invadopodium-based tumor cell invasion and metastatic spread of tumor cells. Furthermore, we determined that the function of Stx4 can be disrupted by ectopic expression of a GFP-tagged peptide fragment comprising the first 15 amino acids of Stx4. With effects similarly to those of the Stx4 cytoplasmic domain, or the Stx4-N-term, the Stx4-1-15 fragment exerts its effects by binding Munc18c and competitively inhibiting the interaction of endogenous Stx4 and Munc18c, leading to impairment of trafficking of MT1-MMP and ECM degradation. The importance of MT1-MMP trafficking was

underscored here by the observation that expression of a mutant form of MT1-MMP (MT1-MMP-T567E), which exhibits accelerated trafficking, partly restored the *in vitro* invasive capacity of cells with a deficit in Stx4-mediated trafficking.

Invadopodia have been well studied as important subcellular structures contributing to ECM invasion in some cancers, and this is supported by analyses of invasive tumors isolated from patients (4), but there does not currently exist a clinical treatment targeting invadopodia-mediated metastasis (4). ABL kinase inhibitors have been shown to decrease invadopodium formation *in vitro*, and MMP-mediated invasiveness in a mouse xenograft model (8). It has also been shown that microRNA miR-182 can inhibit invadopodium formation in human non–small lung cell cancer (NSCLC; ref. 36). Neither of these lines of investigation, however, have progressed to the clinical setting. As well, specifically targeting MMP activity to combat metastatic cancer has proved to be challenging, with many candidate inhibitors failing in clinical trials (37). Thus, alternative strategies to target MMP-driven tumor metastasis need to be considered.

Overall, the work described here elucidates an important molecular mechanism, specifically the regulation of Stx4 by Munc18c, which regulates MT1-MMP activity during the metastatic cascade. This regulatory mechanism may be a suitable target around which therapeutic strategies can be developed. Our results suggest that biological or chemical inhibitors that target the interaction of Stx4 and Munc18c, possibly based on the Stx4-derived peptide fragment used here, hold potential as a therapeutic strategy.

Authors' Disclosures

P.C. McDonald reports grants from Cancer Research Society; and grants from Canadian Institutes of Health Research during the conduct of the study; in addition, P.C. McDonald declares common shares in SignalChem Lifesciences Corporation; and is an inventor on patent US9962398 assigned to Welichem Biotech, Inc. Z.J. Gerbec reports grants from Cancer Research Society; and grants from Canadian Institutes of Health Research during the conduct of the study. W.S. Brown reports grants from Cancer Research Society; and grants from Canadian Institutes of Health Research during the conduct of the study. S. Dedhar reports grants from Cancer Research Society and grants from Canadian Institutes for Health Research during the conduct of the study; in addition, S. Dedhar declares shares in Signal Chem Lifesciences Corp; and is an inventor on patent US9962398, assigned to Welichem Biotech, Inc. M.G. Coppolino reports grants from Cancer Research Society during the conduct of the study. No disclosures were reported by the other authors.

Authors' Contributions

M.I. Brasher: Conceptualization, data curation, formal analysis, investigation, methodology, writing–original draft. **S.C. Chafe:** Data curation, formal analysis, investigation, writing–review and editing. **P.C. McDonald:** Data curation, formal analysis, investigation, writing–review and editing. **O. Nemirovsky:** Data curation, formal analysis, investigation, writing–review and editing. **G. Gorshtein:** Data curation, investigation, writing–review and editing. **Z.J. Gerbec:** Investigation. **W.S. Brown:** Investigation. **O.R. Grafinger:** Data curation, formal analysis, investigation, writing–review and editing. **M. Marchment:** Investigation. **E. Matus:** Investigation. **S. Dedhar:** Resources, funding acquisition, visualization, writing–original draft, writing–review and editing. **M.G. Coppolino:** Conceptualization, resources, supervision, funding acquisition, visualization, writing–original draft, project administration, writing–review and editing.

Acknowledgments

This work was supported by a Cancer Research Society operating grant to M.G. Coppolino, supporting M.I. Brasher, G. Gorshtein, O.R. Grafinger, M. Marchment, and E. Matus; and by operating grants to S. Dedhar, from the Canadian Institutes of Health Research and Cancer Research Society, supporting S.C. Chafe, P. C. McDonald, O. Nemirovsky, Z.J. Gerbec, and W.S. Brown. We acknowledge the land on which the University of Guelph resides is the ancestral lands of the Attawandaron people, and the treaty lands and territory of the Mississaugas of the Credit First Nation, and offer our respect to the Indigenous people that reside there.

The costs of publication of this article were defrayed in part by the payment of page charges. This article must therefore be hereby marked *advertisement* in accordance with 18 U.S.C. Section 1734 solely to indicate this fact.

Received June 10, 2020; revised November 18, 2020; accepted November 24, 2021; published first December 6, 2021.

References

1. Gupta GP, Massagué J. Cancer metastasis: building a framework. Cell 2006;127:679–95.
2. Steeg PS. Tumor metastasis: mechanistic insights and clinical challenges. Nat Med 2006;12:895–904.
3. Steeg PS. Targeting metastasis. Nat Rev Cancer 2016;16:201–18.
4. Meirson T, Gil-Henn H. Targeting invadopodia for blocking breast cancer metastasis. Drug Resist Updat 2018;39:1–17.
5. Lee A, Djamgoz MBA. Triple negative breast cancer: emerging therapeutic modalities and novel combination therapies. Cancer Treat Rev 2018;62:110–22.
6. Gelmon K, Dent R, Mackey JR, Laing K, McLeod D, Verma S. Targeting triple-negative breast cancer: optimising therapeutic outcomes. Ann Oncol 2012;23:2223–34.
7. Hanahan D, Weinberg RA. Hallmarks of cancer: the next generation. Cell 2011;144:646–74.
8. Meirson T, Genna A, Lukic N, Makhnii T, Alter J, Sharma VP, et al. Targeting invadopodia-mediated breast cancer metastasis by using ABL kinase inhibitors. Oncotarget 2018;9:22158–83.
9. Kelly T, Mueller SC, Yeh Y, Chen WT. Invadopodia promote proteolysis of a wide variety of extracellular matrix proteins. J Cell Physiol 1994;158:299–308.
10. Artym VV, Swatkoski S, Matsumoto K, Campbell CB, Petrie RJ, Dimitriadis EK, et al. Dense fibrillar collagen is a potent inducer of invadopodia via a specific signaling network. J Cell Biol 2015;208:331–50.
11. Ondrej T, Rosel D, Vesely P, Folk P, Brabek J. The structure of invadopodia in a complex 3D environment. Eur J Cell Biol 2010;89:674–80.
12. Kumar S, Das A, Barai A, Sen S. MMP secretion rate and inter-invadopodia spacing collectively govern cancer invasiveness. Biophys J 2018;114:650–62.
13. Yamaguchi H. Pathological roles of invadopodia in cancer invasion and metastasis. Eur J Cell Biol 2012;91:902–7.
14. Clark ES, Brown B, Whigham AS, Kochaishvili A, Yarbrough WG, Weaver AM. Aggressiveness of HNSCC tumors depends on expression levels of cortactin, a gene in the 11q13 amplicon. Oncogene 2009;28:431–44.
15. Lohmer LL, Kelley LC, Hagedorn EJ, Sherwood DR. Invadopodia and basement membrane invasion in vivo. Cell Adhes Migr 2014;8:246–55.
16. Eckert MA, Lwin TM, Chang AT, Kim J, Danis E, Ohno-Machado L, et al. Twist1-induced invadopodia formation promotes tumor metastasis. Cancer Cell 2011;19:372–86.
17. Poincloux R, Lizárraga F, Chavrier P. Matrix invasion by tumour cells: a focus on MT1-MMP trafficking to invadopodia. J Cell Sci 2009;122:3015–24.
18. Chen YA, Scheller RH. Snare-mediated membrane fusion. Nat Rev Mol Cell Biol 2001;2:98–106.
19. Williams KC, McNeilly RE, Coppolino MG. SNAP23, Syntaxin4, and vesicle-associated membrane protein 7 (VAMP7) mediate trafficking of membrane type 1–matrix metalloproteinase (MT1-MMP) during invadopodium formation and tumor cell invasion. Mol Biol Cell 2014;25:2061–70.
20. Kean MJ, Williams KC, Skalski M, Myers D, Burtnik A, Foster D, et al. VAMP3, syntaxin-13 and SNAP23 are involved in secretion of matrix metalloproteinases, degradation of the extracellular matrix and cell invasion. J Cell Sci 2009;122:4089–98.
21. Brasher MI, Martynowicz DM, Grafinger OR, Hucik A, Shanks-Skinner E, Uniacke J, et al. Interaction of Munc18c and syntaxin4 facilitates invadopodium formation and extracellular matrix invasion of tumor cells. J Biol Chem 2017;292:16199–210.
22. Hong W. SNAREs and traffic. Biochim Biophys Acta 2005;1744:120–44.

23. Yu H, Rathore SS, Lopez JA, Davis EM, James DE, Martin JL, et al. Comparative studies of Munc18c and Munc18–1 reveal conserved and divergent mechanisms of Sec1/Munc18 proteins. Proc Natl Acad Sci U S A 2013;110:E3271–80.
24. Latham CF, Lopez JA, Hu SH, Gee CL, Westbury E, Blair DH, et al. Molecular dissection of the Munc18c/Syntaxin4 interaction: implications for regulation of membrane trafficking. Traffic 2006;7:1408–19.
25. Williams KC, Coppolino MG. Phosphorylation of membrane type 1-matrix metalloproteinase (MT1-MMP) and its vesicle-associated membrane protein 7 (VAMP7)-dependent trafficking facilitate cell invasion and migration. J Biol Chem 2011;286:43405–16.
26. Lou Y, Preobrazhenska O, auf dem Keller U, Sutcliffe M, Barclay L, McDonald PC, et al. Epithelial-mesenchymal transition (EMT) is not sufficient for spontaneous murine breast cancer metastasis. Dev Dyn 2008;237:2755–68.
27. Hoover H, Muralidharan-Chari V, Tague S, D'Souza-Schorey C. Investigating the role of ADP-ribosylation factor 6 in tumor cell invasion and extracellular signal-regulated kinase activation. Methods Enzymol 2005;404:134–47.
28. Williams KC, Coppolino MG. SNARE-dependent interaction of Src, EGFR and β1 integrin regulates invadopodia formation and tumor cell invasion. J Cell Sci 2014;127:1712–25.
29. Enot DP, Vacchelli E, Jacquelot N, Zitvogel L, Kroemer G. TumGrowth: an open-access web tool for the statistical analysis of tumor growth curves. Oncoimmunology 2018;7:e1462431.
30. Acharyya S, Oskarsson T, Vanharanta S, Malladi S, Kim J, Morris PG, et al. A CXCL1 paracrine network links cancer chemoresistance and metastasis. Cell 2012;150:165–78.
31. Leong HS, Robertson AE, Stoletov K, Leith SJ, Chin CA, Chien AE, et al. Invadopodia are required for cancer cell extravasation and are a therapeutic target for metastasis. Cell Rep 2014;8:1558–70.
32. Oh E, Spurlin BA, Pessin JE, Thurmond DC. Munc18c heterozygous knockout mice display increased susceptibility for severe glucose intolerance. Diabetes 2005;54:638–47.
33. Thurmond DC, Kanzaki M, Khan AH, Pessin JE. Munc18c function is required for insulin-stimulated plasma membrane fusion of GLUT4 and insulin-responsive amino peptidase storage vesicles. Mol Cell Biol 2000;20:379–88.
34. Tamori Y, Kawanishi M, Niki T, Shinoda H, Araki S, Okazawa H, et al. Inhibition of insulin-induced GLUT4 translocation by Munc18c through interaction with syntaxin4 in 3T3-L1 adipocytes. J Biol Chem 1998;273:19740–6.
35. Thurmond DC, Ceresa BP, Okada S, Elmendorf JS, Coker K, Pessin JE. Regulation of insulin-stimulated GLUT4 translocation by Munc18c in 3T3L1 adipocytes. J Biol Chem 1998;273:33876–83.
36. Li Y, Zhang H, Gong H, Yuan Y, Li Y, Wang C, et al. miR-182 suppresses invadopodia formation and metastasis in non-small cell lung cancer by targeting cortactin gene. J Exp Clin Cancer Res 2018;37:141.
37. Vandenbroucke RE, Libert C. Is there new hope for therapeutic matrix metalloproteinase inhibition? Nat Rev Drug Discov 2014;13:904–27.